

The Effects of DOPO-g-ITA Modified Microcrystalline Cellulose on the Properties of Composite Phenolic Foams

Yufeng Ma¹, Xuanang Gong¹ and Puyou Jia^{2,*}

¹Nanjing Forestry University, College of Materials Science and Engineering, Co-Innovation Center of Efficient Processing and Utilization of Forest Resources, Nanjing, 210037, China

²Institute of Chemical Industry of Forestry Products, CAF, Nanjing, 210042, China

*Corresponding Author: Puyou Jia. Email: jiapuyou@icifp.cn

Received: 16 September 2019; Accepted: 31 October 2019

Abstract: In order to improve the comprehensive performance of phenolic foam, 9, 10-dihydro-9-oxa-10-phosphaphenanthrene-10-oxide (DOPO) was grafted with itaconic acid (ITA) (DOPO-g-ITA) to modify microcrystalline cellulose (MCC). DOPO-g-ITA modified MCC (DIMMCC) was used to prepare composite phenolic foam (DCPF). The structures of DIMMCC were verified by Fourier transform infrared spectroscopy (FT-IR). The microstructure and crystalline property were characterized by scanning electron microscope (SEM) and X-ray diffraction (XRD) respectively. Compared with MCC, the crystallinity of DIMMCC was dramatically decreased, but the diffraction peak positions were unchanged. Thermal stability was decreased, and T_i decreased by 45.0°C. The residual carbon (600°C) was increased by 22.34%. With the dosage of DIMMCC/PR increased, compared with PF, the mechanical properties and flame retardancy of DCPF were increased. Especially, the dosage of DIMMCC/PR was 10%, the comprehensive properties of DCPF was better than others.

Keywords: DOPO; ITA; MCC; phenolic foams; composites

1 Introduction

Phenolic foam (PF) offers excellent flame retardant, low smoke and toxicity, and as a thermal insulation material, which is widely used in the field of aviation, construction, industrial pipelines and transportation [1-3]. However, due to its fragility, large-scale promotion and application are greatly restricted [3-5]. In order to improve the performance of PF, the toughening modification of PF is imperative.

As a renewable and environmentally friendly natural macromolecular resource, cellulose offers low cost and density, high specific strength, degradable, non-toxic and good mechanical properties, which has become one of the most concerned polymer reinforcing materials [6-9]. Microcrystalline cellulose (MCC) is a kind of purified and partially depolymerized cellulose, where the amorphous regions of cellulose are removed by acid hydrolysis, which occurs as a white, odorless, tasteless, crystalline powder composed of porous particles, and can be a very promising cellulosic reinforcement for polymers [10]. At present, MCC is used in various fields such as pharmacy, cosmetics, food industry, and plastics processing industry [10, 11]. Nevertheless, MCC is a non-flame retardant material, which is utilized in the field of the composites to improve the mechanical properties without reducing its flame retardancy, the flame retardant modification of MCC is required.



This work is licensed under a Creative Commons Attribution 4.0 International License, which permits unrestricted use, distribution, and reproduction in any medium, provided the original work is properly cited.

9, 10-dihydro-9-oxa-10-phosphaphenanthrene-10-oxide (DOPO) is an excellent flame retardant [12]. There is very active phosphor hydrogen bond in its chemical structure, the nucleophilic addition reaction is easy occurred. Therefore DOPO has attracted extensive attention in the field of flame retardant polymers [13-18]. Itaconic acid (ITA) is an important renewable unsaturated dicarboxylic acid. Due to conjugacy relation between unsaturated bond and one carboxy, ITA has a strong reaction capacity, which can be used to synthesize polymers by the addition, esterification or polymerization reactions, and is widely utilized in the field of synthetic fibers, resins, adhesives, etc. [19-22]. Therefore, this study aims to introduce DOPO into the structure of ITA, and then DOPO-g-ITA is used to modify MCC, Finally, the modified MCC is utilized to prepare the composite PF. DOPO and ITA are chosen due to their versatilities in organic synthesis [20-24]. It was hypothesized that it could not only enhance the mechanical properties of composite PF, but also without reducing the flame retardancy.

In this study, the structure, crystallinity, thermal stability and microstructure of DOPO-g-ITA modified MCC (DIMMCC) was characterized by fourier transform infrared spectroscopy (FT-IR), X-ray diffraction (XRD), scanning electron microscope (SEM) and thermal gravimetric analyzer (TGA). The mechanical and fragile properties, flame resistance and microstructure of DIMMCC composite PF (DCPF) were investigated as well.

2 Materials and Methods

2.1 Materials

Phenol (> 99%), formaldehyde (37 wt%), calcium oxide (CaO), sodium hydroxide (NaOH), dimethylformamide and potassium carbonate (K_2CO_3) were obtained from Nanjing Chemical Reagent, Ltd. 9, 10-dihydro-9-oxa-10-phosphaphenanthrene-10-oxide (DOPO) and itaconic acid (ITA) were purchased from Aladdin. Polysorbate-80, petroleum ether, xylene, tetrahydrofuran, microcrystalline cellulose (MCC) and Paraformaldehyde ($\geq 95\%$) were obtained from Sinopharm group Chemical Reagent Co. Ltd. mixed acid curing agent were obtained from Institute of Chemical Industry of Forestry Products, Chinese Academy of Forestry.

2.2 Preparation of DOPO-g-ITA Modified MCC (DIMMCC)

Synthesis and characterization of DOPO-g-ITA was according to the literature [25]. MCC (0.28 mmol), DOPO-g-ITA (0.125 mol), K_2CO_3 (0.01 mol) and dimethylformamide (60 ml) were added into a round bottom flask fitted with magnetic stirring, the reaction was performed for 9 h at $120^\circ C$. And then the vacuum filtration and absterion were performed three times, DIMMCC was obtained and after drying to a constant weight at $50^\circ C$ in a vacuum oven. The synthesis scheme of DIMMCC was shown in Fig. 1.



Figure 1: Scheme of DIMMCC

2.3 Preparation of Phenolic Resin (PR) and Composite PFs

Phenol (2.0 mol) and formaldehyde (0.5 mol) were charged into a 1000 ml four-necked round bottom flask fitted with stirrer and condenser, and a calculated amount of CaO (0.015 mol) was dropped

slowly into the vessel for 30–40 min under continuously stirring at 90°C. The first part of paraformaldehyde (1.75 mol) and NaOH aqueous solution (50%, 0.3 mol) were then added into the reactor and reacted at 90°C for 50–70 min. Then the second part of paraformaldehyde (1.75 mol) and NaOH aqueous solution (50%, 0.3 mol) was added and reacted at 85°C for 50–70 min. Finally the third part of NaOH aqueous solution (50%, 0.15 mol) was added to the reactor and the reaction was performed temperature at 75°C for 15–20 min. PR could be obtained.

Surfactants (Polysorbate-80, 5%/PR), acid curing agents (20%/PR), DIMMCC (5 wt%/PR, 10 wt%/PR, 15 wt%/PR and 20 wt%/PR) and blowing agents (petroleum ether, 5%/PR) were added into PR and completely mixed by mechanical stirrer, which was then poured into a mold. Phenolic foams were obtained after foaming for 40 min at 70°C.

2.4 Characterizations

FT-IR spectra of DIMMCC were monitored by a Fourier transform infrared spectrometer (Nicolet IS10, America). XRD spectra of DIMMCC were collected on a Shimadzu 6000X X-ray diffractometer. SEM were used to observe the micro-scale morphology of DIMMCC and PFs by a Hitachi S3400-Scanning electron microscope. Thermogravimetric analysis (TGA) curves were collected by a NETZCSH TG 209 F3 TGA system under nitrogen atmosphere. Samples were heated from 35 to 600°C at a heating rate of 10°C/min. Compression strength, bending strength and tensile strength were measured according to the standard ISO 844:2014, ISO 1209-1:2012 and ISO 1926-2009, respectively. Limiting oxygen indexes (LOIs) of all samples were obtained at room temperature on a JF-3 LOI instrument (LOI analysis instrument company, Jiangning County, China) according to ISO 4589-1-2017.

3 Results and Discussion

3.1 FT-IR Spectra of DOPO-g-ITA Modified MCC (DIMMCC)

Figure 2 shows FT-IR spectra of DIMMCC. the FT-IR analysis of DOPO-g-ITA [25]: 1704 cm^{-1} (C=O); 1608 cm^{-1} , 1595 cm^{-1} and 1581 cm^{-1} (phenyl); 1429 cm^{-1} (P-phenyl), 1245 cm^{-1} (P=O), 913 cm^{-1} (P-O-phenyl). The FT-IR analysis of MCC [26-31]: 3343 cm^{-1} (-OH); 2902 cm^{-1} (CH); 1645 cm^{-1} (H_2O), 1432 cm^{-1} (CH_2), 1058 cm^{-1} , 1031 cm^{-1} (C-O-C); 895 cm^{-1} (CH of β -glucosides). The FT-IR analysis of DIMMCC: 3330 cm^{-1} (-OH); 2894 cm^{-1} (CH); 1433 cm^{-1} (CH_2), 1053 cm^{-1} , 1019 cm^{-1} (C-O-C). Compared with the FT-IR spectrum of MCC, the characteristic peak of OH was significantly reduced at 3330 cm^{-1} . And several new characteristic peaks were observed in the FT-IR spectrum of

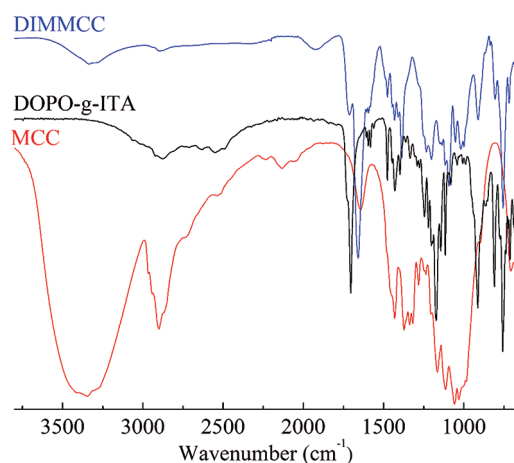


Figure 2: FT-IR spectra of DIMMCC

DIMMCC. 1712 cm^{-1} (C=O of ester bond); 1606 cm^{-1} , 1594 cm^{-1} and 1580 cm^{-1} (phenyl) 1429 cm^{-1} (P-phenyl), 1232 cm^{-1} (P=O), 911 cm^{-1} (P-O-phenyl) [25, 32-34]. From the FT-IR analysis, it was indicated that the esterification reaction occurred between DOPO-g-ITA and MCC, DOPO-g-ITA was successfully introduced in the molecular structure of MCC.

3.2 XRD Curves of DIMMCC

As shown in Fig. 3, the main diffraction peaks of DIMMCC and MCC were located at approximately 15.0° , 16.6° , 22.8° and 34.6° , which corresponded to the 110, 110, 002, and 040 planes, and the crystalline structure of DIMMCC and MCC was corresponded to cellulose I crystal [35-37]. Compared with MCC, the diffraction peak positions of DIMMCC were unchanged, despite the significantly attenuation of the peak intensity. The result showed that the crystal structure of DIMMCC was not destroyed, because DOPO-g-ITA was covered on the surface of MCC by modification, which led to the significant decrease of the crystallinity of DIMMCC.

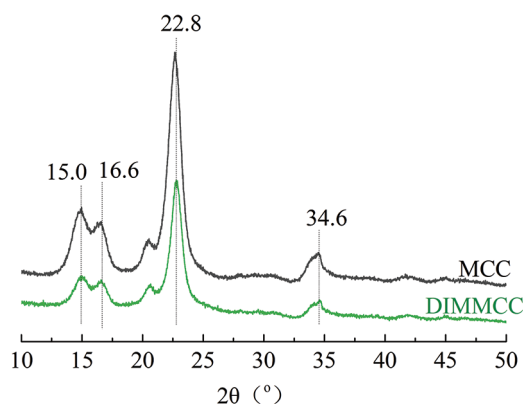


Figure 3: XRD curves of DIMMCC

3.3 The Microstructure of DIMMCC

Figure 4 shows SEM micrographs ($1000\times$) of DIMMCC and MCC. The surface of MCC was very rough, and has lots of weeny wrinkles. Compared with MCC, the surface of DIMMCC was smoother, and was covered by a thin layer of material. This might be explained that after modification, the esterification reaction was occurred between DOPO-g-ITA and MCC. DOPO-g-ITA was introduced in the molecular structure of MCC. Finally, the surface of MCC was covered by DOPO-g-ITA.

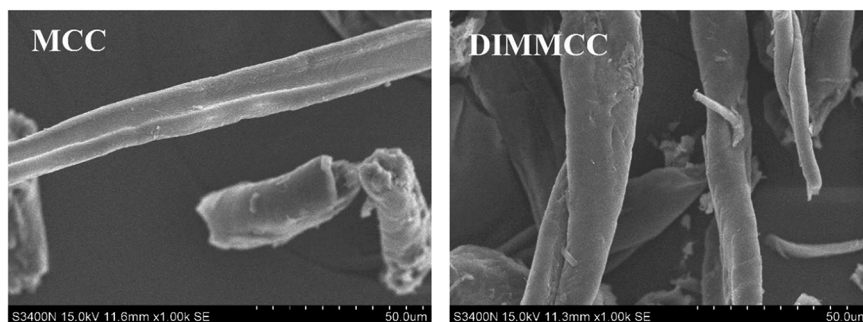


Figure 4: SEM of DIMMCC

3.4 TG and DTG Curves of DIMMCC

TG and DTG of DIMMCC was shown in Fig. 5. The initial decomposition temperatures (T_i) [38] of DIMMCC, MCC and DOPO-g-ITA were 286.0°C, 331.0°C and 152.9°C respectively, and the carbon residue (600°C) were 29.58%, 7.24% and 10.51% respectively. It was observed that T_i of DIMMCC was less than that of MCC, but the carbon residue (600°C) of DIMMCC was more than that of MCC. It might be explained that T_i (152.9°C) of DOPO-g-ITA was less than that of MCC, Therefore, there was no positive significance to improve the heat resistance of DIMMCC. However, the carbon residue (600°C) (10.51%) of DOPO-g-ITA was more than that of MCC; Otherwise, biphenyls heterocycle was introduced in the structure of DIMMCC after modification, and increased the carbon content of DIMMCC. Thus, the carbon residue (600°C) of DIMMCC was remarkably improved.

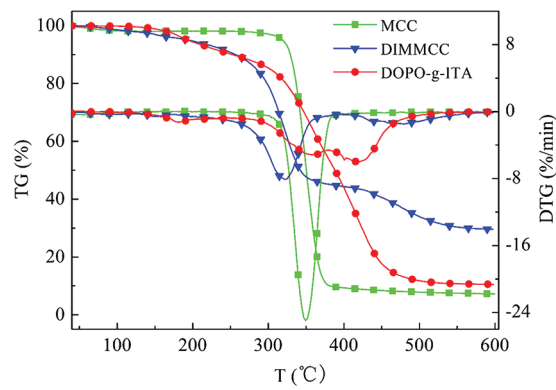


Figure 5: TG and DTG curves of DIMMCC

3.5 Compression and Bending Strength of DIMMCC Composite PF(DCPF)

As shown in Fig. 6, With the increasing of the dosage of DIMMCC/PR, the compression and bending strength of DCPF were gradually increased firstly, then decreased, and were more than that of PF. When the dosage of DIMMCC/PR was 10%, compression and bending strength were the largest of all the foams. It might be explained by that DIMMCC was introduced into PF, the toughness of DCPF was improved. Therefore, the ability of resistance bending was increased and significantly better than that of PF. However, when the dosage of DIMMCC was more, the cell structures of DCPF were destroyed and the mechanical properties of DCPF were deteriorated. Therefore, the suitable dosage of DIMMCC/PR was no more than 10%.

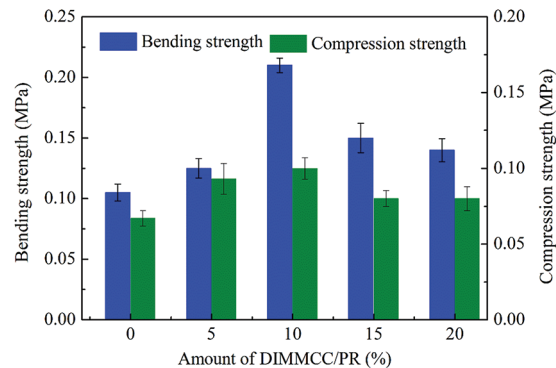


Figure 6: Compression and Bending strength of DCPF

3.6 Tensile Strength of DCPF

Tensile strength of DCPF was shown in Fig. 7. When the amount of DIMMCC/PR was no more than 10%, tensile strength of DCPF was gradually increased, and was more than that of PF. Then tensile strength of DCPF were gradually decreased, and were less than that of PF. The result indicated that a small amount of DIMMCC introduced was beneficial to improve the mechanical properties of DCPF, and the ability of resistance tensile deformation was slightly improved. However, when the content of DIMMCC/PR was more, which caused a reduction in mechanical properties of DCPF. It might be explained that after DIMMCC introduced in DCPF, When the foam was subjected to tensile stress, the resin matrix could be dragged by DIMMCC, which was similar to the effect of steel bars in concrete, so tensile strength of DCPF was gradually increased, and was more than that of PF. Nevertheless, with increasing amount of DIMMCC/PR, the mechanical properties of DCPF was enhanced improved along with the destroy of the cell structures of DCPF increased. There should be a balance between toughening and breaking. When the amount of DIMMCC/PR was no more than 10%, toughening was in the ascendant compared with breaking. Therefore, the tensile strength of DCPF was more than that of PF. Then breaking was in the ascendant, the tensile strength of DCPF was less than that of PF. Thus, the suitable dosage of DIMMCC/PR was no more than 10%.

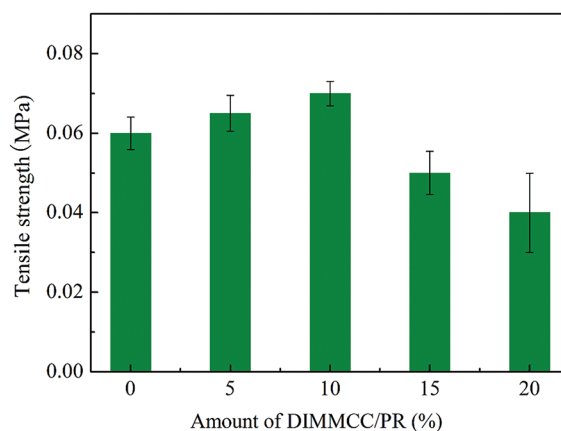


Figure 7: Tensile strength of DCPF

3.7 Fragility of DCPF

Fragility is often used to characterize the toughness of foams, which is commonly represented with the mass loss rate. The greater mass loss rate will cause the better toughness of foams [39-41]. Fig. 8 shows the fragility of DCPF. The result revealed that with the dosage of DIMMCC/PR increased, the mass loss rate was decreased, then was increased. When the dosage of DIMMCC/PR was 10%, the mass loss rate of DCPF was the lowest in all of samples, and was less than that of PF, others were more than that of PF. The reason might be explained that with the increasing dosage of DIMMCC/PR, the original bubble structure was destroyed and the bubble uniformity was decreased, which led to the mass loss rate increased. Otherwise, the toughness of DCPF was improved by the introduction of DIMMCC. There should be a balance between toughening and breaking. When toughening was in the ascendant, the mass loss rate of DCPF was less than that of PF, instead was more than that of PF. The results showed that the dosage of DIMMCC/PR was not too much, the better dosage of DIMMCC/PR was 10%.

3.8 Limited Oxygen Index (LOI) of DCPF

As shown in Fig. 9, LOI of DCPF was gradually increased with the dosage of DIMMCC/PR increased. and were more than that of PF. And these foams were considered as the flame resistant materials ($LOI \geq 27\%$) [42]. The results showed that LOI of DCPF was distinctly improved by the introduction of DIMMCC. This

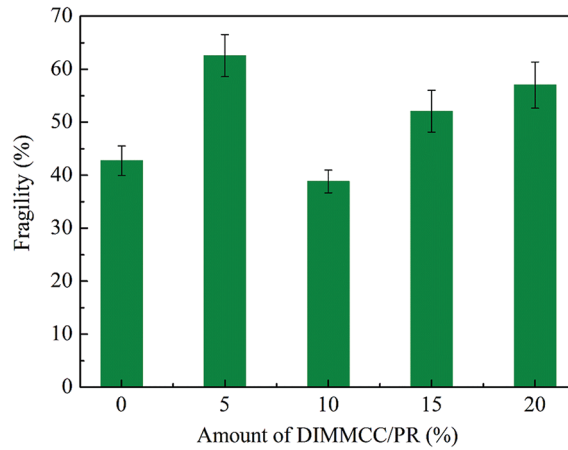


Figure 8: Fragility of DCPF

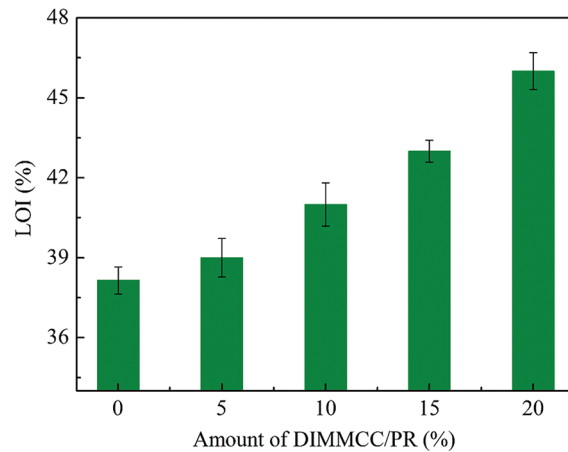


Figure 9: LOI of DCPF

might be explained by that the phosphorus element (in DIMMCC) was introduced into DCPF, during the process of combustion, the fire retardant quenching effect could be exerted by releasing free PO radicals and terminating the chain reaction of combustion in gas phase [12]. Therefore, LOI of DCPF was more than that of PF. And with the increasing of DIMMCC/PR, there was more flame retardants introduced into DCPF, LOI was improved dramatically.

3.9 The Microstructure of DCPF

SEM micrographs (50 \times) of DCPF are showed in Fig. 10. The cell size of PF was about at 200~500 μm . With the content of DIMMCC/PR increased, the cell size of DCPF was decreased slightly, then was increased gradually. And the number of large cells was increased. When the dosage of DIMMCC/PR was 10%, the cell size of DCPF was the smallest in all of samples, which was less than that of PF, and was about at 120~400 μm . When the dosage of DIMMCC/PR was 10%, the structure of cells was relatively small and regular. Therefore, the negative influence of DIMMCC on the properties of DCPF was less neglected and the mechanical properties of DCPF were better.

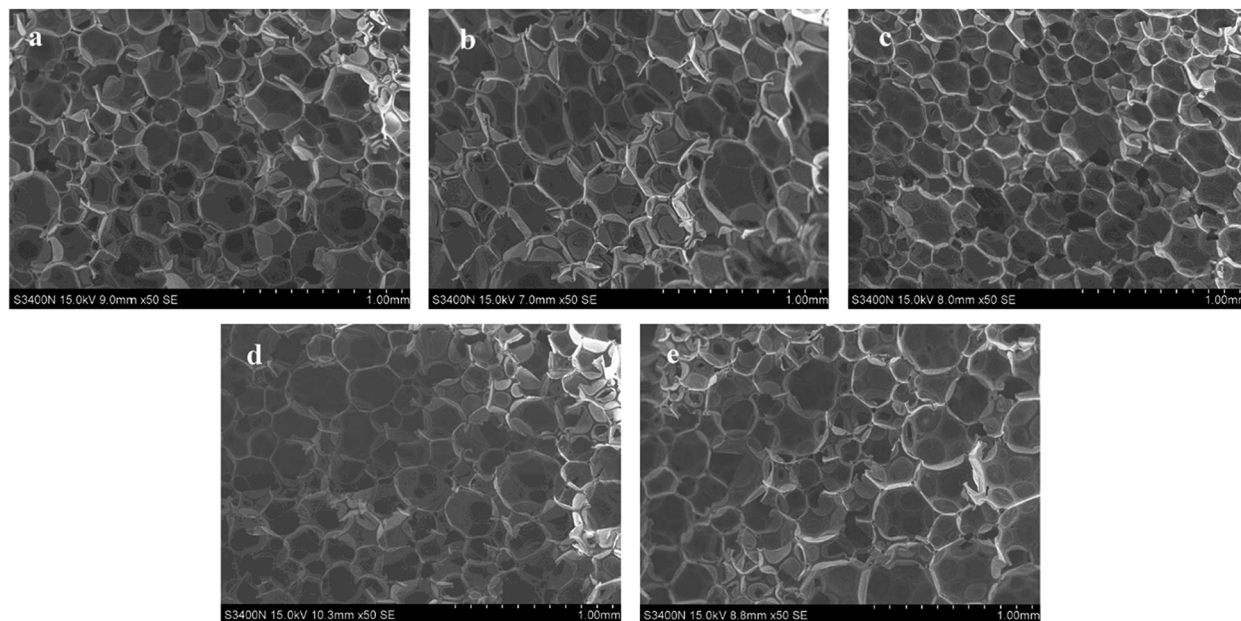


Figure 10: SEM of DCPF (a:0%; b:5%; c:10%; d:15%; e:20%)

4 Conclusions

The structure of DIMMCC was confirmed by FT-IR. The esterification reaction between DOPO-g-ITA and MCC was verified by FT-IR spectra and SEM, DOPO-g-ITA was successfully introduced in the molecular structure of MCC. Compared with MCC, the crystallinity of DIMMCC was dramatically decreased and the diffraction peak positions were unchanged. Additionally, T_i of DIMMCC decreased, but the residual carbon (600°C) increased significantly. With the dosage of DIMMCC/PR increased, the mechanical properties and flame retardancy of DCPF were increased. When the dosage of DIMMCC/PR was 10%, the comprehensive properties of DCPF was better than others.

Acknowledgements: The work was partially financially supported by The Youth Innovation Fund of Nanjing Forestry University (CX2016011); Nanjing Forestry University High-Level (High-Educated) Talents Scientific Research Funds (GXL2014033); The authors would like to acknowledge for the support on this research and the Analytical and Testing Center for the help of measurement.

Conflicts of Interest: The authors declare that they have no conflicts of interest to report regarding the present study.

References

1. Yang, H., Wang, X., Yuan, H., Song, L., Hu, Y. et al. (2012). Fire performance and mechanical properties of phenolic foams modified by phosphorus-containing polyethers. *Journal of Polymer Research*, 19(3), 9831. DOI 10.1007/s10965-012-9831-7.
2. Lei, S., Guo, Q., Zhang, D., Shi, J., Liu, L. et al. (2010). Preparation and properties of the phenolic foams with controllable nanometer pore structure. *Journal of Applied Polymer Science*, 117(6), 3545–3550.
3. Auad, M. L., Zhao, L., Shen, H., Nutt, S. R., Sorathia, U. (2010). Flammability properties and mechanical performance of epoxy modified phenolic foams. *Journal of Applied Polymer Science*, 104(3), 1399–1407. DOI 10.1002/app.24405.

4. Rangari, V. K., Hassan, T. A., Zhou, Y., Mahfuz, H., Jeelani, S. et al. (2010). Cloisite clay-infused phenolic foam nanocomposites. *Journal of Applied Polymer Science*, *103*(1), 308–314. DOI 10.1002/app.25287.
5. Ma, Y., Wang, C., Chu, F. (2017). Effects of fiber surface treatments on the properties of wood fiber-phenolic foam composites. *Bioresources*, *12*(3), 4722–4736.
6. Mulinari, D. R., Voorwald, H. J., Cioffi, M. O., da Silva, M. L. C. P. (2016). Cellulose fiber-reinforced high-density polyethylene composites—mechanical and thermal properties. *Journal of Composite Materials*, *51*(13), 1807–1815. DOI 10.1177/0021998316665241.
7. Luo, Q., Li, Y., Pan, L., Song, L., Yang, J. et al. (2016). Effective reinforcement of epoxy composites with hyperbranched liquid crystals grafted on microcrystalline cellulose fibers. *Journal of Materials Science*, *51*(19), 1–12. DOI 10.1007/s10853-015-9500-4.
8. Pérez-Fonseca, A. A., Robledo-Ortíz, J. R., González-Núñez, R., Rodrigue, D. (2016). Effect of thermal annealing on the mechanical and thermal properties of polylactic acid-cellulosic fiber biocomposites. *Journal of Applied Polymer Science*, *133*(31), 43750.
9. Wang, H., Zhang, J., Wang, W., Wang, Q. (2016). Research of fiber reinforced wood-plastic composites: a review. *Scientia Silvae Sinicae*, *52*(6), 130–139.
10. Mathew, A. P., Oksman, K., Sain, M. (2010). Mechanical properties of biodegradable composites from poly lactic acid (PLA) and microcrystalline cellulose (MCC). *Journal of Applied Polymer Science*, *97*(5), 2014–2025. DOI 10.1002/app.21779.
11. Adel, A. M., El-Wahab, Z. H. A., Ibrahim, A. A., Al-Shemy, M. T. (2011). Characterization of microcrystalline cellulose prepared from lignocellulosic materials. Part II: Physicochemical properties. *Carbohydrate Polymers*, *83*(2), 676–687.
12. Tang, S., Qian, L., Qiu, Y., Dong, Y. (2018). Synergistic flame-retardant effect and mechanisms of boron/phosphorus compounds on epoxy resins. *Polymers for Advanced Technologies*, *29*(1), 641–648. DOI 10.1002/pat.4174.
13. Zhang, W., Li, X., Yang, R. (2011). Novel flame retardancy effects of DOPO-POSS on epoxy resins. *Polymer Degradation and Stability*, *96*(12), 2167–2173. DOI 10.1016/j.polymdegradstab.2011.09.016.
14. Zang, L., Wagner, S., Ciesielski, M., Müller, P., Döring, M. (2011). Novel star-shaped and hyperbranched phosphorus-containing flame retardants in epoxy resins. *Polymers for Advanced Technologies*, *22*(7), 1182–1191. DOI 10.1002/pat.1990.
15. Dumitrascu, A. (2012). Flame retardant polymeric materials achieved by incorporation of styrene monomers containing both nitrogen and phosphorus. *Polymer Degradation and Stability*, *97*(12), 2611–2618. DOI 10.1016/j.polymdegradstab.2012.07.012.
16. Sun, D., Yao, Y. (2011). Synthesis of three novel phosphorus-containing flame retardants and their application in epoxy resins. *Polymer Degradation and Stability*, *96*(10), 1720–1724. DOI 10.1016/j.polymdegradstab.2011.08.004.
17. Wang, P., Cai, Z. (2017). Highly efficient flame-retardant epoxy resin with a novel DOPO-based triazole compound: thermal stability, flame retardancy and mechanism. *Polymer Degradation & Stability*, *137*, 138–150. DOI 10.1016/j.polymdegradstab.2017.01.014.
18. Perret, B., Schartela, B., Ciesielski, M., Diederichs, J., Döring, M. et al. (2011). Novel DOPO-based flame retardants in high-performance carbon fibre epoxy composites for aviation. *European Polymer Journal*, *47*(5), 1081–1089. DOI 10.1016/j.eurpolymj.2011.02.008.
19. Li, Z., Zhuang, Z. L., Wu, W. B., Dai, H. Q. (2016). Preparation of cellulose-g-PNIPAAm copolymers by atom transfer radical polymerization. *Transactions of China Pulp & Paper*, *31*(1), 41–46.
20. Dai, J., Ma, S., Wu, Y., Han, L., Zhang, L. et al. (2015). Polyesters derived from itaconic acid for the properties and bio-based content enhancement of soybean oil-based thermosets. *Green Chemistry*, *17*(4), 2383–2392. DOI 10.1039/C4GC02057J.
21. Winkler, M., Lacerda, T. M., Mack, F., Meier, M. A. R. (2015). Renewable polymers from itaconic acid by polycondensation and ring-opening-metathesis polymerization. *Macromolecules*, *48*(5), 1398–1403. DOI 10.1021/acs.macromol.5b00052.

22. Kamzolova, S. V., Allayarov, R. K., Lunina, J. N., Morgunov, I. G. (2016). The effect of oxalic and itaconic acids on threo-Ds-isocitric acid production from rapeseed oil by *Yarrowia lipolytica*. *Bioresource Technology*, 206, 128–133. DOI 10.1016/j.biortech.2016.01.092.
23. Carja, I. D., Serbezeanu, D., Vladbubulac, T., Hamciuc, C., Coroaba, A. et al. (2014). A straightforward, eco-friendly and cost-effective approach towards flame retardant epoxy resins. *Journal of Materials Chemistry A*, 2(38), 16230–16241. DOI 10.1039/C4TA03197K.
24. Dong, Q., Ding, Y., Wen, B., Wang, F., Dong, H. et al. (2012). Improvement of thermal stability of polypropylene using DOPO-immobilized silica nanoparticles. *Colloid and Polymer Science*, 290(14), 1371–1380. DOI 10.1007/s00396-012-2631-0.
25. Ma, Y., Gong, X., Liao, C., Geng, X., Wang, C. et al. (2018). Preparation and characterization of DOPO-ITA modified ethyl cellulose and its application in phenolic foams. *Polymers*, 10(10), 1049. DOI 10.3390/polym10101049.
26. Haafiz, M. M., Eichhorn, S., Hassan, A., Jawaid, M. (2013). Isolation and characterization of microcrystalline cellulose from oil palm biomass residue. *Carbohydrate Polymers*, 93(2), 628–634. DOI 10.1016/j.carbpol.2013.01.035.
27. Kian, L. K., Jawaid, M., Ariffin, H., Alothman, O. Y. (2017). Isolation and characterization of microcrystalline cellulose from roselle fibers. *International Journal of Biological Macromolecules*, 103, 931–940. DOI 10.1016/j.ijbiomac.2017.05.135.
28. Bahluli, R., Keshipour, S. (2019). Microcrystalline cellulose modified with Fe(II)- and Ni(II)-phthalocyanines: syntheses, characterizations, and catalytic applications. *Polyhedron*, 169, 176–182. DOI 10.1016/j.poly.2019.05.010.
29. Keshipour, S., Khezerloo, M. (2019). Nanocomposite of hydrophobic cellulose aerogel/graphene quantum dot/Pd: synthesis, characterization, and catalytic application. *RSC Advances*, 9(30), 17129–17136. DOI 10.1039/C9RA01799B.
30. Keshipour, S., Khezerloo, M. (2018). Au-dimercaprol functionalized cellulose aerogel: synthesis, characterization and catalytic application. *Applied Organometallic Chemistry*, 32(4), e4255. DOI 10.1002/aoc.4255.
31. Keshipour, S., Adak, K. (2017). Magnetic d-penicillamine-functionalized cellulose as a new heterogeneous support for cobalt(II) in green oxidation of ethylbenzene to acetophenone. *Applied Organometallic Chemistry*, 31(11), e3774. DOI 10.1002/aoc.3774.
32. Lin, C. H., Wu, C. Y., Wang, C. S. (2015). Synthesis and properties of phosphorus-containing advanced epoxy resins. II. *Journal of Applied Polymer Science*, 78(1), 228–235.
33. Zhang, C., Huang, J. Y., Liu, S. M., Zhao, J. Q. (2011). The synthesis and properties of a reactive flame-retardant unsaturated polyester resin from a phosphorus-containing diacid. *Polymers for Advanced Technologies*, 22(12), 1768–1777. DOI 10.1002/pat.1670.
34. Songqi, M. A., Liu, X. Q., Jiang, Y. H., Fan, L. B., Feng, J. X. et al. (2014). Synthesis and properties of phosphorus-containing bio-based epoxy resin from itaconic acid. *Science China Chemistry*, 57(3), 379–388.
35. Kian, L. K., Jawaid, M., Ariffin, H., Karim, Z. (2018). Isolation and characterization of nanocrystalline cellulose from roselle-derived microcrystalline cellulose. *International Journal of Biological Macromolecules*, 114, 54–63. DOI 10.1016/j.ijbiomac.2018.03.065.
36. Bai, C., Huang, X., Xie, F., Xiong, X. (2018). Microcrystalline cellulose surface-modified with acrylamide for reinforcement of hydrogels. *ACS Sustainable Chemistry & Engineering*, 6(9), 12320–12327. DOI 10.1021/acssuschemeng.8b02781.
37. Huang, X., Xie, F., Xiong, X. (2018). Surface-modified microcrystalline cellulose for reinforcement of chitosan film. *Carbohydrate Polymers*, 201, 367–373. DOI 10.1016/j.carbpol.2018.08.085.
38. Chen, T., Chen, X., Wang, M., Hou, P., Jie, C. et al. (2017). A novel halogen-free co-curing agent with linear multi-aromatic rigid structure as flame-retardant modifier in epoxy resin. *Polymers for Advanced Technologies*, 29(1), 603–611. DOI 10.1002/pat.4170.
39. Ma, Y., Geng, X., Zhang, X. (2018). Effect of novel DOPO-g-Coupling agent treated wood fibers on properties of composite phenolic foams. *BioResources*, 13(3), 6187–6200.

40. Ma, Y., Geng, X., Zhang, X., Wang, C., Chu, F. (2019). Synthesis of DOPO-g-GPTS modified wood fiber and its effects on the properties of composite phenolic foams. *Journal of Applied Polymer Science*, 136(2), 46917. DOI 10.1002/app.46917.
41. Ma, Y., Geng, X., Zhang, X., Wang, C., Chu, F. (2018). A novel DOPO-g-KH550 modification wood fibers and its effects on the properties of composite phenolic foams. *Polish Journal of Chemical Technology*, 20(2), 47–53. DOI 10.2478/pjct-2018-0022.
42. Wang, C., Xu, G. (2010). Research on hard-segment flame-retardant modification of waterborne polyurethane. *China Coatings*, 25(8), 57–60.